[CANCER RESEARCH 60, 4556–4560, August 15, 2000]

Tumor Oxygenation in Hormone-Dependent Tumors During Vascular Endothelial Growth Factor Receptor-2 Blockade, Hormone Ablation, and Chemotherapy[1]

Nils Hansen-Algenstaedt, Brian R. Stoll, Timothy P. Padera, Dennis E. J. G. J. Dolmans, Daniel J. Hicklin, Dai Fukumura, and Rakesh K. Jain[2]

Edwin L. Steele Laboratory, Department of Radiation Oncology, Massachusetts General Hospital and Harvard Medical School, Boston, MA 02114 [N. H., B. R. S., T. P. P., D. E. J. G. J. D., D. F., R. K. J.]; Department of Chemical Engineering [B. R. S.], Massachusetts Institute of Technology, and Division of Health Sciences and Technology [T. P. P.], Massachusetts Institute of Technology and Harvard Medical School, Cambridge, MA 02139; Department of Immunology, ImClone Systems Incorporated, New York, NY, 10014 [D. J. H.]

ABSTRACT

Tumor oxygenation is critical for tumor survival as well as for response to therapy, *e.g.*, radiation therapy. Hormone ablation therapy in certain hormone-dependent tumors and antiangiogenic therapy lead to vessel regression and have also shown beneficial effects when combined with radiation therapy. These findings are counterintuitive because vessel regression should reduce oxygen tension (pO_2) in tumors, decreasing the effectiveness of radiotherapy. Here we report on the dynamics of pO_2 and oxygen consumption in a hormone-dependent tumor following hormone ablation and during treatment with an anti-VEGFR-2 monoclonal antibody (mAb) or a combination of doxorubicin and cyclophosphamide; the latter combination is not known to cause vessel regression at doses used clinically. Androgen-dependent male mouse mammary carcinoma (Shionogi) was implanted into transparent dorsal skin-fold chambers in male severe combined immunodeficient mice. Thirteen days after the tumors were implanted, mice were treated with antiangiogenic therapy (anti-VEGFR-2 mAb, 1.4 mg/30 g body weight), hormone ablation by castration, or doxorubicin (6.5 mg/kg every 7 days) and cyclophosphamide (100 mg/kg every 7 days). A non-invasive *in vivo* method was used to measure pO_2 profiles and to calculate oxygen consumption rates (Q_{O2}) in tumors. Tumors treated with anti-VEGFR-2 mAb exhibited vessel regression and became hypoxic. Initial vessel regression was followed by a "second wave" of angiogenesis and increases in both pO_2 and Q_{O2}. Hormone ablation led to tumor regression followed by an increase in pO_2 coincident with regrowth. Chemotherapy led to tumor growth arrest characterized by constant Q_{O2} and elevated pO_2. The increased pO_2 during anti-VEGFR-2 mAb and hormone ablation therapy may explain the observed beneficial effects of combining antiangiogenic or hormone therapies with radiation treatment. Thus, understanding the microenvironmental dynamics is critical for optimal scheduling of these treatment modalities.

INTRODUCTION

Solid tumors are typically characterized by hypoxia (1–3). Despite continuous angiogenesis, local disparities between the rate of oxygen supplied by the blood and the oxygen consumption rate (Q_{O2})[3] of the tissue leave large numbers of cells in a state of oxygen deprivation. Some of these hypoxic tumor cells remain viable and contribute to the resistance of tumors to radiotherapy and to some anti-neoplastic drugs. As a result, therapies that affect the tumor environment have become a major focus in cancer research (3, 4). The hypoxic tumor microenvironment is a stimulus for angiogenesis, up-regulating expression of angiogenic factors such as vascular endothelial growth factor (VEGF) by tumor (5) and stromal (6) cells. VEGF is a potent angiogenic factor that promotes proliferation of tumor vascular endothelium and increases vascular permeability (7, 8). Thus, therapies that neutralize or interfere with VEGF signaling should cause vessel regression and inhibit growth (*e.g.*, Refs. 8–12). One would also expect these therapies to increase hypoxia in tumors and limit the effectiveness of radiation and certain drug therapies. Surprisingly, the combination of angiogenesis inhibitors and radiotherapy or chemotherapy has led to additive or synergistic tumor response[4] (13–15). Similarly, hormone ablation in hormone-dependent tumors, which leads to impaired vascular function (9), has shown synergistic effects when used in combination with radiation therapy (16).

Understanding the dynamics of tumor oxygenation during tumor regression and relapse is, thus, crucial for optimal scheduling of combined treatment (1, 2). Separate measurements of the partial pressure of oxygen (pO_2) and Q_{O2} have been made in tumors and, in limited cases, during response to therapy[4] (4, 17). However, noninvasive measurements of pO_2 profiles (and calculation of Q_{O2}) during treatment have not been reported. Here we quantify for the first time temporal changes in tumor pO_2 and Q_{O2} in response to antiangiogenic, hormone ablation, or chemotherapy (doxorubicin/cyclophosphamide). Androgen-dependent Shionogi tumors were grown in transparent dorsal skin-fold chambers in severe combined immunodeficient mice. The transparent chamber model allowed us to visualize tumor growth, regression, and relapse-over extended periods (18) and to non-invasively measure tissue pO_2 using the recently developed phosphorescence quenching microscopy (PQM) technique (2).

MATERIALS AND METHODS

Tumor Model and Treatment. Male severe combined immunodeficient mice from our gnotobiotic colony were implanted with transparent dorsal skin-fold chambers (18). Androgen-dependent male mouse mammary carcinoma (Shionogi) was implanted 3 days after chamber implantation as described previously (9). Intravital microscopy was performed every third day to document tumor growth and vascularization (18). Because tumor size is an important determinant of therapeutic outcome, treatment was initiated 13 days following tumor implantation, after the tumors had become established and had developed a functional vascular network. Mice in the antiangiogenic group received either anti-VEGFR-2 monoclonal antibody (mAb; DC101, 45 mg/kg, i.p.; Ref. 19) or an equal amount of non-specific rat IgG (Jackson Immunochemicals, West Grove, PA) every 3 days. Mice in the chemotherapy group received either doxorubicin (6.5 mg/kg, i.p.) and cyclophosphamide (100 mg/kg, i.p.) or an equal amount of physiological saline every 7 days. Mice in the hormone ablation group underwent either an orchiectomy (9) or a sham operation. All procedures were carried out following approval of the Institutional Animal Care and Use Committee.

Tumor Growth Analysis. The growth data were described using the rectilinear form of the Gompertz equation (20): $\ln[\ln A_{max} - \ln A(t)] = \ln\beta/\alpha - \alpha t$,

Received 11/23/99; accepted 6/21/00.

The costs of publication of this article were defrayed in part by the payment of page charges. This article must therefore be hereby marked *advertisement* in accordance with 18 U.S.C. Section 1734 solely to indicate this fact.

[1] Supported by National Cancer Institute Outstanding Investigator Grant R35-CA 56591 (to R. K. J). N. H-A. was a recipient of a Deutsche Forschungsgemeinschaft Research Fellowship (HA 2790/1-1). T. P. P. was a recipient of a National Science Foundation Graduate Pre-Doctoral Fellowship.

[2] To whom requests for reprints should be addressed, at Department of Radiation Oncology, Massachusetts General Hospital, Boston, MA 02114. Phone: (617) 726-4083; Fax: (617) 726-4172; E-mail: jain@steele.mgh.harvard.edu.

[3] The abbreviations used are: Q_{O2}, oxygen consumption rate; VEGF, vascular endothelial growth factor; pO_2, partial pressure of oxygen; PQM, phosphorescence quenching microscopy; mAb, monoclonal antibody.

[4] C. G. Lee, M. Heijn, E. di Tomaso, G. Griffon-Etienne, M. Ancukiewicz, C. Koike, K. R. Park, N. Ferrara, R. K. Jain, H. D. Suit, and Y. Boucher. Anti-VEGF treatment augments tumor radiation response under normoxic or hypoxic conditions, in press.

which relates tumor cross-sectional area (A) to time (t). The parameters (α, β) were determined by comparing this model to the experimental growth data using a linear regression.

Vessel Volume per Area. The vascular volume per unit area was calculated based on the vessel diameter (D) and length (L):

$$\text{volume per area} = \frac{\pi}{4A}\sum_{i=1}^{M} D_i^2 L_i$$

where M is the total number of vessels in the region with the area A (11). The vessel diameter and length were measured in five distinct regions (each ≈0.5 mm in length) using image analysis of the tumor vasculature.

Phosphorescence Quenching Microscopy. High resolution PQM was used to measure pO_2 profiles (2). Tissue pO_2 was measured between adjacent vessels in 20-μm increments. Briefly, albumin-bound palladium *meso*-tetra-(4-carboxyphenyl) porphyrin (Medical Systems Corp., Greenvale, NY) was injected i.v. via the tail vein (60 mg/kg). Three to seven fields of view were selected randomly throughout the tumor. After 30 min, excitation was generated by flashes ($n \leq 15$) from a 540-nm flashlamp (EG&G, Salem, MA). Phosphorescence signals (≥630 nm; Oriel, Stratford, CT) were detected with a photomultiplier tube (9203B, Products for Research, Danvers, MA), averaged on a digital oscilloscope (TDS-320, Tektronix, Beaverton, OR), and transferred to a computer. Lifetime constants (τ) were obtained from this data and pO_2 values were calculated using the Stern-Volmer equation, $pO_2 = 1/k(1/\tau - 1/\tau_0)$ (21). In this expression, k and τ_0 are the quenching constant and the phospho-rescence lifetime in the absence of oxygen, respectively. To establish pre-treatment values, oxygen levels were measured on day 12, 1 day before initiating therapy. After initiating therapy, oxygen levels were measured 14, 20, 26, and 32 days after tumor implantation. RBC velocity was also measured in these vessels using the temporal correlation velocimetry described elsewhere (19).

Oxygen Consumption Rate. To estimate changes in Q_{O2} with time, a one-dimensional linear diffusion-reaction model was used: $DSd_x^2C - Q_{O2} = 0$, where D = diffusion coefficient, S = oxygen solubility, $C = pO_2$, x = distance from the vessel, and Q_{O2} = constant consumption rate. Using the boundary conditions, $C(0) = C_0$ and $d_xC|_{x=x_{crit}} = 0$, where x_{crit} is the distance from the vessel at which the minimum pO_2 (minimum concentration, C_{min}) is measured, gives the solution

$$C(x) = (Q_{O2}/2DS)x^2 - \sqrt{2Q_{O2}(C_0 - C_{min})/DS}\,x + C_0.$$

pO_2 data were fit with this second order polynomial. We assumed a value of $D = 2 \times 10^{-5}$ cm^2/s (22), $S = 2.05 \times 10^{-5}$ ml$_{O2}$/cm^3 · mm Hg (23), and calculated Q_{O2} (ml$_{O2}$/cm^3 · min). Q_{O2} were calculated only for those vessels that were greater than 200 μm from the nearest neighboring vessel to satisfy the assumptions in the mathematical model.

Statistical Analysis. Results are presented as mean ± SE. ANOVA tests were performed to compare the equality of controls. F-tests were used to test the equality of variances. Two sample t-tests for independent samples of equal variances were performed to compare sample means. Statistical significance was based on P values smaller than 5%. Prior to the first day of treatment (day 13), there were no statistically significant differences between the four groups (control, anti-VEGFR-2 mAb, hormone ablation, and doxorubicin/cyclophosphamide) included in the study.

RESULTS

Tumor size and transformed tumor size analyzed using the rectilinear form of the Gompertz model are shown in Fig. 1, *A* and *B*, respectively. Tumors in the control groups exhibited similar growth curves, independent of the treatment modality (saline, non-specific IgG, or sham operation). Hormone ablation and treatment with doxorubicin/cyclophosphamide resulted in significant growth delays ($P < 0.05$). The growth of the anti-VEGFR-2 mAb-treated group was not significantly different from the control group. The growth data were used to ensure that comparisons of pO_2 and Q_{O2} values were size-matched because tumor size is known to be an important determinant of oxygenation (24).

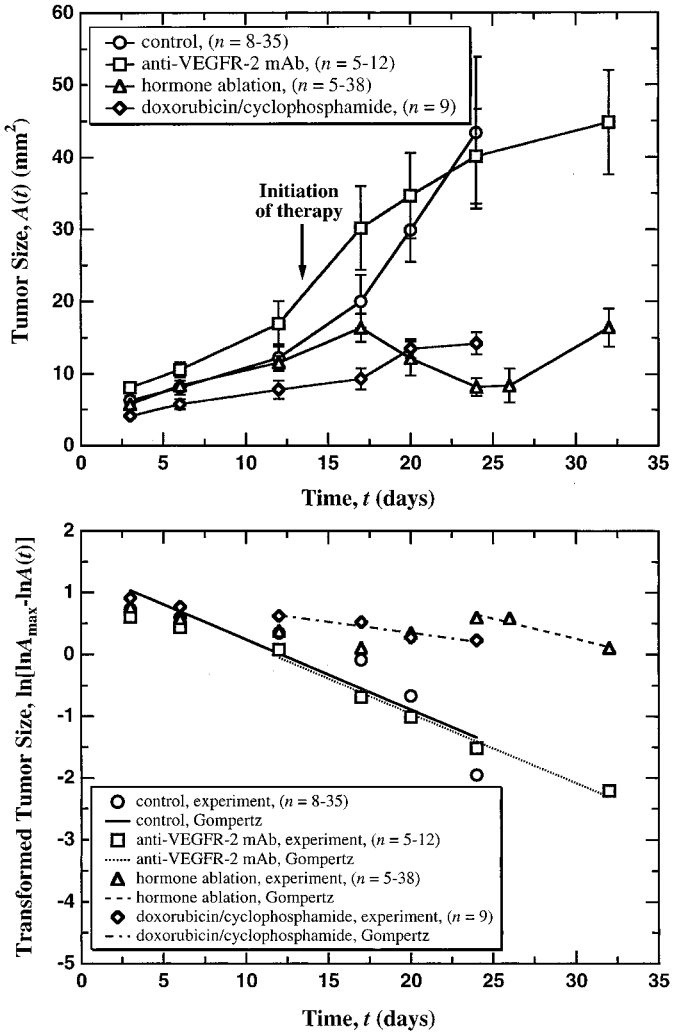

Fig. 1. Tumor growth. *A*, Tumor size (mm^2) is plotted as a function of time. *B*, Transformed tumor size is plotted as a function of time. Transformed tumor size was calculated using the rectilinear form of the Gompertz model and the data were fit using a linear regression. Tumor growth data were used to ensure size-matched comparisons of pO_2 and Q_{O2} values.

Fig. 2 shows a representative set of pO_2 data and the corresponding fit of the data to the diffusion-reaction equation used to calculate Q_{O2}.

Established solid tumors with a functional vascular network were most oxygenated (mean ± SE = 22 ± 3 mm Hg) 14 days after tumor implantation (Fig. 3*A*). When tumors became larger, tumor oxygenation decreased. On day 26 when control tumors reached the size of the dorsal chamber, tumor oxygenation decreased further to values of about 11 ± 2 mm Hg. In contrast to tumor pO_2, oxygen consumption rate remained constant throughout the entire experiment in control tumors (Fig. 3*E*), indicating that for this tumor, oxygenation is size-dependent but Q_{O2} is not.

The first effect of anti-VEGFR-2 mAb on tumor pO_2 occurred within 24 h of initiating treatment. Compared with size-matched controls (22 ± 2 mm Hg), a significant ($P < 0.05$) drop in pO_2 occurred in the anti-VEGFR-2 mAb (15 ± 1 mm Hg) group. Vessel volume per unit area remained constant during this time (Fig. 4). One week after initiation of therapy, pO_2 values decreased further to 10.2 ± 1.9 mm Hg ($P < 0.05$, 41% decrease compared with size-matched controls; Fig. 3*B*). The decrease in pO_2 was accompanied by a significant ($P < 0.05$) decrease in vessel volume per unit area (Fig. 4), though Q_{O2} remained unaffected (Fig. 3*F*). Vessel volume per unit

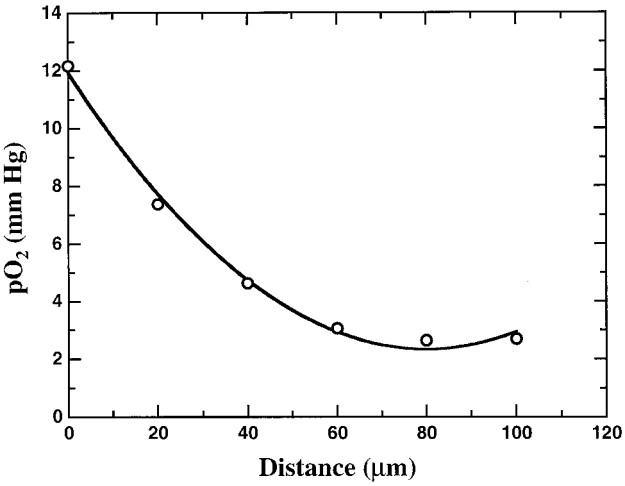

Fig. 2. Calculation of Q_{O2}. The figure shows a representative set of pO_2 values and the corresponding fit of the data to the diffusion-reaction equation. The data show the change in pO_2 moving away from the wall of a blood vessel in an anti-VEGFR-2 mAb-treated tumor on day 14. pO_2 measurements were made using PQM.

area decreased over days 20–26 and reached a minimum after day 26, 13 days after initiation of anti-VEGFR-2 mAb treatment. At this point, vessels appeared less tortuous (Fig. 5*A*). Despite the decrease in vessel volume per unit area, pO_2 levels did not further decrease below 10 mm Hg. Approximately 3 weeks after initiating anti-VEGFR-2 mAb treatment, increased vessel volume per unit area was observed (Figs. 4 and 5*A*), accompanied by increased pO_2 (137% compared with size-matched controls) and Q_{O2} (Fig. 3, *B* and *F*).

Changes in pO_2 and Q_{O2} following hormone ablation mirrored two distinct stages of tumor vascularization: regression and regrowth. Analogous to anti-VEGFR-2 mAb therapy, pO_2 values dropped significantly ($P < 0.05$) compared with size-matched controls within 24 h of hormone ablation (from 22 ± 2 to 15 ± 2 mm Hg). Tumor and vessel regression (Fig. 5*B*) occurred 1 week after hormone ablation, during which there was an increase in tumor pO_2 to 23 ± 2 mm Hg ($P < 0.05$, 30% compared with size-matched controls; Fig. 3*D*), likely the result of a decrease in oxygen demand. The maximum tumor regression (Fig. 1*A*) and minimum Q_{O2} (Fig. 3*H*) with constant pO_2 (22 ± 2 mm Hg) coincided on day 26. Tumor regression was followed by tumor relapse after day 26 accompanied by a "second wave" of angiogenesis (Fig. 5*B*) and an increase in Q_{O2} (Fig. 3*H*). Despite the increase in Q_{O2}, pO_2 levels remained higher ($P < 0.05$, 51% compared with size-matched controls) in the treatment group.

Doxorubicin/cyclophosphamide induced tumor growth arrest without regression and did not significantly affect tumor oxygenation or Q_{O2}. Tumor oxygenation remained constant at 22 ± 2 mm Hg during the first week of treatment (day 14 to day 20). Two weeks after treatment, tumors exhibited a slight decrease to 16 ± 2 mm Hg ($P < 0.05$, 13% less compared with size-matched controls; Fig. 3*C*). Q_{O2} remained unchanged throughout the entire experiment (Fig. 3*G*).

DISCUSSION

The importance of low oxygen in cancer treatment response has been discussed since the description of tumor hypoxia by Thomlinson and Gray (25). To improve existing therapies and to develop new strategies, it is essential to understand how various tumor therapies influence the local microenvironment. Because tumor pO_2 fluctuates, reflecting the imbalance between oxygen supply and Q_{O2}, a continuous, controlled, non-invasive *in vivo* analysis is necessary to gain insight into the dynamics of tumor oxygenation (2).

Oxygen tension in all control groups decreased with increasing tumor size despite increases in vessel density. Q_{O2}, on the other hand, remained constant, indicating unchanged metabolic demands. This implicates hindered oxygen delivery as the cause of tumor hypoxia. This is supported by the observation that pO_2 at the vessel wall decreases with increasing tumor size. The decrease in delivery could be attributable to increased consumption by endothelial cells (26, 27), impaired oxygen carrying capacity, or increased oxygen extraction from blood as it flows over longer distances through the growing tumor.

The decrease in pO_2 observed 1 day after initiating treatment in the

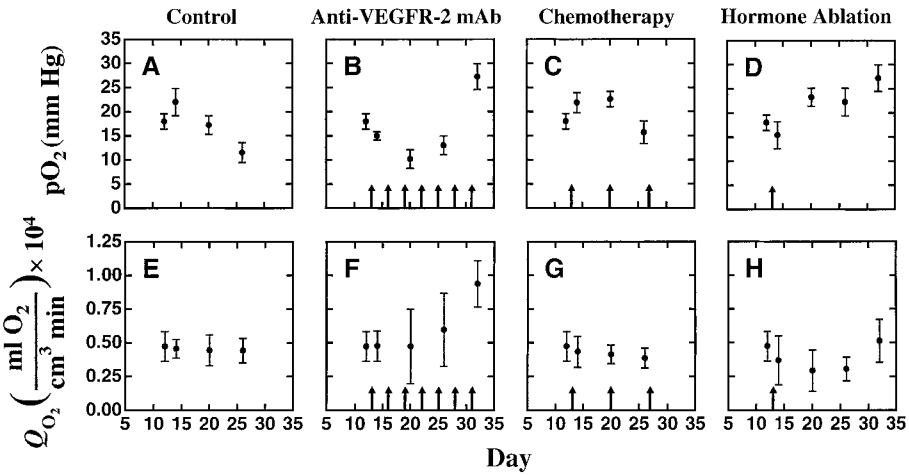

Fig. 3. Mean pO_2 (*A–D*) pO_2 measurements. Measurements were taken in tissue in 20-μm increments moving away from the vessel wall. Arrows indicate days on which treatment was administered. *A*, Control (n = 4–17, vessel diameter = 60.6 ± 10.2 μm; mean ± SE). Controls consisted of saline-injected, IgG-injected, and sham-operated animals, with no significant difference among control groups (ANOVA). pO_2 decreased from day 14 to 26 as tumor size increased. *B*, Anti-VEGFR-2 mAb therapy (n = 4–8, vessel diameter = 45.1 ± 7.9 μm). pO_2 decreased ($P < 0.05$) initially after treatment (day 14) until day 20. pO_2 increased ($P < 0.05$) from day 26 to 32, associated with a second wave of angiogenesis. *C*, Doxorubicin/cyclophosphamide therapy (n = 4–5, vessel diameter = 36.2 ± 6.9 μm). pO_2 was greater ($P < 0.05$) than control from day 14 until day 20. pO_2 was less than control on day 26. *D*, Hormone ablation (n = 4–5, vessel diameter = 50.3 ± 8.5 μm). pO_2 was greater ($P < 0.05$) than control for day 20 through day 32. Note that all comparisons of pO_2 were made based on size-matched controls. *E–H*, Oxygen consumption rates. *E*, Control (n = 4–17, vessel diameter = 60.6 ± 10.2 μm). Controls consisted of saline-injected, IgG-injected, and sham-operated animals, with no significant difference among control groups (ANOVA). Q_{O2} did not change throughout the observation period. *F*, Anti-VEGFR-2 mAb therapy (n = 4–8, vessel diameter = 45.1 ± 7.9 μm). Q_{O2} significantly increases ($P < 0.05$) from day 14 to 32. *G*, Doxorubicin/cyclophosphamide therapy (n = 4–5, vessel diameter = 36.2 ± 6.9 μm). Q_{O2} in growth-arrested tumors remained constant. *H*, Hormone ablation (n = 4–5, vessel diameter = 50.3 ± 8.5 μm). A decreasing trend ($P = 0.11$) in Q_{O2} was observed between days 14 and 26. An increasing trend ($P = 0.15$) in Q_{O2} was observed between days 26 and 32.

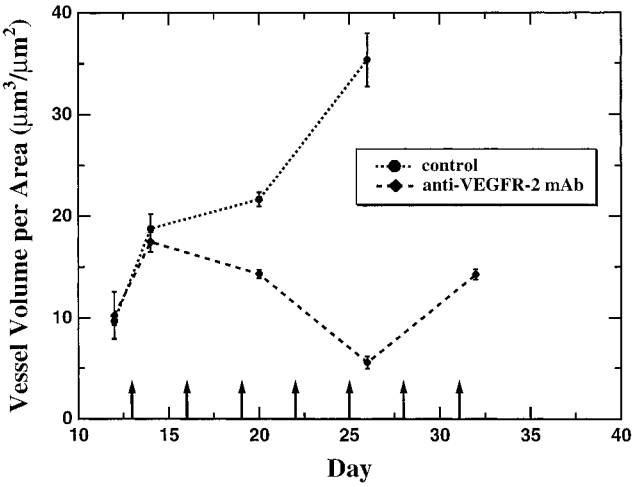

Fig. 4. Vascular density (n = 3–5). Volumetric vessel density is plotted against time. Anti-VEGFR-2 mAb therapy caused a dramatic reduction in volumetric vessel density after day 20 as compared with controls. The arrow indicates administration of antibody.

hormone ablation and anti-VEGFR-2 mAb groups is likely the result of the ability of these treatments to alter vascular function by inducing endothelial cell apoptosis (9) or by blocking VEGF signaling. In both treatments, the subsequent period of low pO_2 is followed by increases in pO_2 and Q_{O2}, coincident with a second wave of angiogenesis. In the anti-VEGFR-2 mAb-treated group, the high pO_2 levels observed with increases in vasculature and despite increases in Q_{O2} may be the result of increased tissue perfusion. Blood flow rate measurements indicate that RBC velocity during vessel regression and relapse (day 14: V_{RBC} = 74.9 ± 2.1 μm/s; day 20: V_{RBC} = 80.9 ± 1.8 μm/s; day 26: V_{RBC} = 79.7 ± 3.3 μm/s; day 30: V_{RBC} = 72.9 ± 3.1 μm/s; and day 35: V_{RBC} = 75.4 ± 2.1 μm/s) does not change appreciably ($P > 0.23$, one-way ANOVA). However, vessel density increases significantly during the later stages of therapy (after day 26), suggesting improved tissue perfusion. In addition, similar to observations made in studies in which VEGF itself was neutralized (11) or down-regulated (9), vessels that develop during the second wave of angiogenesis appear less tortuous (Fig. 5). The increase in Q_{O2} is presumably due to an increase in the number of oxygen-consuming cells and mirrors the metabolic demands of the tumor. Thus, it appears that Q_{O2}, not pO_2, mirrors the dynamics of tumor growth and regression in agreement with the findings of Gullino *et al.* in tissue-isolated tumors (28).

To investigate the possibility that the second wave of angiogenesis observed during anti-VEGFR-2 mAb therapy may be the result of hypoxia-induced up-regulation of VEGF (9), anti-VEGFR-2 mAb was administered in excess to ensure complete competitive inhibition. The second wave of angiogenesis still occurred under these conditions, suggesting that it may be mediated by alternate signaling pathways or by other angiogenic factors. The mechanisms underlying the second wave of angiogenesis require further investigation.

During doxorubicin/cyclophosphamide therapy there was no sig-

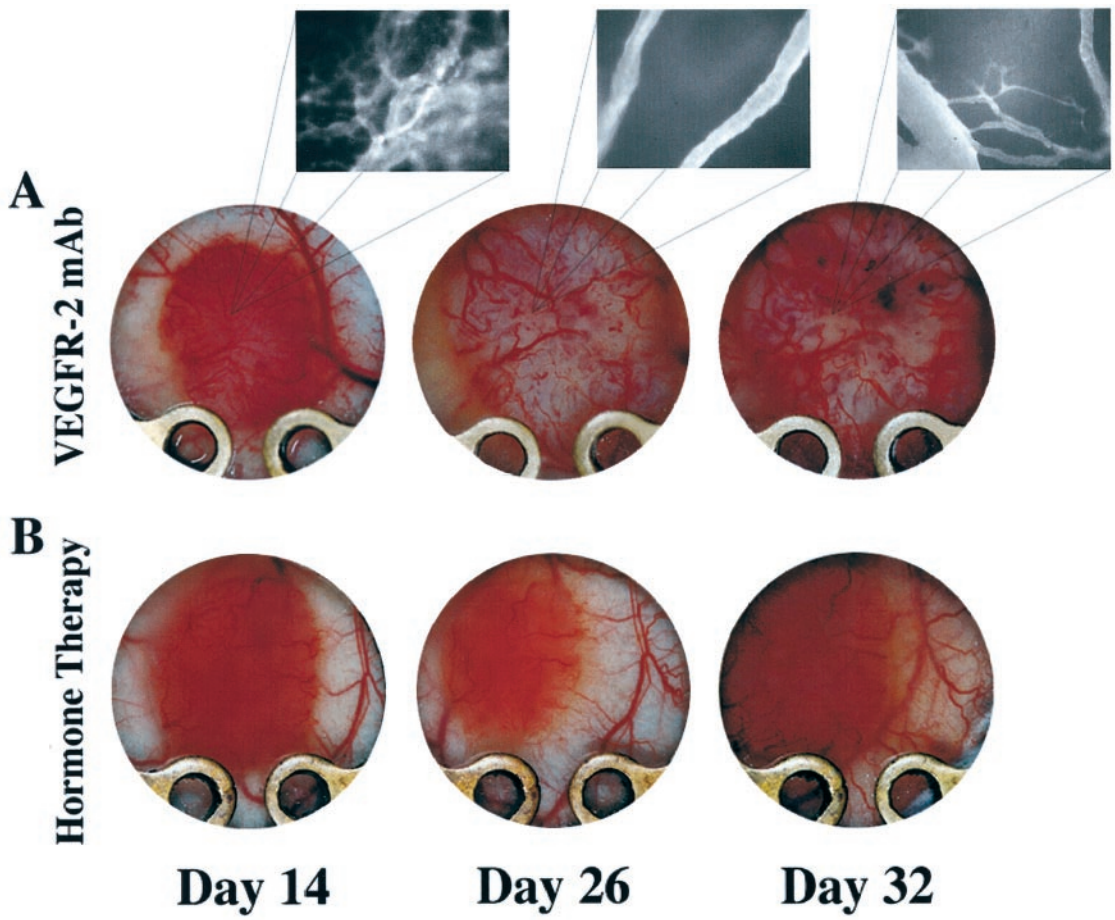

Fig. 5. Photographs of Shionogi tumors grown in dorsal skin-fold chambers were taken 14, 26, and 32 days after the tumors were implanted. Therapy was initiated in well-vascularized tumors on day 13. *A*, Anti-VEGFR-2 mAb therapy. The color photographs show reduced vessel density on day 26 and vessel regrowth on day 32. Black and white images (enlarged views) illustrate changes in vessel morphology following treatment. *B*, Hormone ablation. Tumor regression is visible on day 26 with tumor regrowth and increased vessel density illustrated on day 32.

nificant tumor growth or change in tumor vascularization (data not shown). The constant pO_2 and Q_{O2} levels observed following therapy are compatible with growth arrest during which there is little increase in the number of tumor cells. These findings are consistent with other published observations (17). The slight decrease in tumor oxygenation on day 26 is consistent with the slight increase in tumor size. Compared with size-matched controls, pO_2 did not change. The effectiveness of radiation is enhanced by increased oxygenation and/or reduced tumor volume (29). Because neither a change in Q_{O2} nor an increase in pO_2 (compared with size-matched controls) was observed during chemotherapy, the benefits of combining radiation with chemotherapy are likely not the result of enhanced oxygenation but rather reduced tumor volume (30). Reduced tumor volume is likely the effect of chemotherapy on both tumor cells and endothelial cells (31, 32).

Tumor size and oxygenation are predictors of the success of radiation therapy (1) and chemotherapy (33). The elevated pO_2 resulting from the second wave of angiogenesis in anti-VEGFR-2 mAb therapy and hormone ablation should enhance the effectiveness of oxygen-dependent treatments such as radiation therapy. This finding may help to explain the beneficial effects of combining antiangiogenic and radiation therapy[4] (4, 14). This finding also illustrates the importance of timing in the administration of combined treatments. Following hormone ablation therapy, the second wave of angiogenesis and increase in pO_2 are preceded by tumor regression that is most pronounced 12–14 days after treatment. The effectiveness of radiation therapy is therefore likely to be enhanced just before relapse when tumors exhibit increased pO_2 and decreased size. Indeed, Zietman *et al.* (16) observed radiation therapy to be most effective 12–14 days after hormone ablation. Collectively, these findings point out that understanding the temporal dynamics of tumor oxygenation is necessary in guiding the schedule of combined therapies. The development of PQM allows the temporal dynamics of tumor oxygen tension to be measured non-invasively and chronically. If similar data are used in the clinic to develop optimal scheduling of combined treatment modalities, synergistic effects may be observed in patients.

ACKNOWLEDGMENTS

We thank Y. Boucher, D. Buerk, L. Gerweck, A. Hartford, A. Kadambi, W. Ruether, P. Bohlen, and H.D. Suit for their critical comments. We thank S. Roberge, J. K. Kahn, J. Huber, and A. Santiago for their outstanding technical support.

REFERENCES

1. Vaupel, P., Kallinowski, F., and Okunieff, P. Blood flow, oxygen and nutrient supply, and metabolic microenvironment of human tumors: a review. Cancer Res., *49:* 6449–6465, 1989.
2. Helmlinger, G., Yuan, F., Dellian, M., and Jain, R. K. Interstitial pH and pO_2 gradients in solid tumors *in vivo*: high-resolution measurements reveal a lack of correlation. Nat. Med., *3:* 177–182, 1997.
3. Brown, J. M., and Giaccia, A. J. The unique physiology of solid tumors: opportunities (and problems) for cancer therapy. Cancer Res., *58:* 1408–1416, 1998.
4. Teicher, B. A. Hypoxia and drug resistance. Cancer Metastasis Rev., *13:* 139–168, 1994.
5. Shweiki, D., Itin, A., Soffer, D., and Keshet, E. Vascular endothelial growth factor induced by hypoxia may mediate hypoxia-initiated angiogenesis. Nature (Lond.), *359:* 843–845, 1992.
6. Fukumura, D., Xavier, R., Sugiura, T., Chen, Y., Park, E. C., Lu, N., Selig, M., Nielsen, G., Taksir, T., Jain, R. K., and Seed, B. Tumor induction of VEGF promoter activity in stromal cells. Cell, *94:* 715–725, 1998.
7. Brown, L. F., Detmar, M., Claffey, K., Nagy, J. A., Feng, D., Dvorak, A. M., and Dvorak, H. F. Vascular permeability factor/vascular endothelial growth factor: a multifunctional angiogenic cytokine. *In:* I. D. Goldberg and E. M. Rosen (eds.), Regulation of Angiogenesis, pp. 233–269. Basel, Switzerland: Birkhäuser Verlag, 1997.
8. Ferrara, N., and Davis-Smyth, T. The biology of vascular endothelial growth factor. Endocr. Rev., *18:* 4–25, 1997.
9. Jain, R. K., Safabakhsh, N., Sckell, A., Chen, Y., Jiang, P., Benjamin, L., Yuan, F., and Keshet, E. Endothelial cell death, angiogenesis, and microvascular function after castration in an androgen-dependent tumor: role of vascular endothelial growth factor. Proc. Natl. Acad. Sci. USA, *95:* 10820–10825, 1998.
10. Millauer, B., Shawver, L. K., Plate, K. H., Risau, W., and Ullrich, A. Glioblastoma growth inhibited *in vivo* by a dominant-negative Flk-1 mutant. Nature (Lond.), *367:* 576–579, 1994.
11. Yuan, F., Chen, Y., Dellian, M., Safabakhsh, N., Ferrara, N., and Jain, R. K. Time-dependent vascular regression and permeability changes in established human tumor xenografts induced by an anti-vascular endothelial growth factor/vascular permeability factor antibody. Proc. Natl. Acad. Sci. USA, *93:* 14765–14770, 1996.
12. Prewett, M., Huber, J., Li, Y., Santiago, A., O'Connor, W., King, K., Overholser, J., Hooper, A., Pytowski, B., Witte, L., Bohlen, P., and Hicklin, D. J. Antivascular endothelial growth factor receptor (fetal liver kinase 1) monoclonal antibody inhibits tumor angiogenesis and growth of several mouse and human tumors. Cancer Res., *59:* 5209–5218, 1999.
13. Teicher, B. A., Holden, S. A., Ara, G., Dupuis, N. P., Liu, F., Yuan, J., Ikebe, M., and Kakeji, Y. Influence of an anti-angiogenic treatment on 9L gliosarcoma: oxygenation and response to cytotoxic therapy. Int. J. Cancer, *61:* 732–737, 1995.
14. Mauceri, H. J., Hanna, N. N., Beckett, M. A., Gorski, D. H., Staba, M. J., Stellato, K. A., Bigelow, K., Heimann, R., Gately, S., Dhanabal, M., Soff, G. A., Sukhatme, V. P., Kufe, D. W., and Weichselbaum, R. R. Combined effects of angiostatin and ionizing radiation in antitumour therapy. Nature (Lond.), *394:* 287–291, 1998.
15. Gorski, D. H., Beckett, M. A., Jaskowiak, N. T., Calvin, D. P., Mauceri, H. J., Salloum, R. M., Seetharam, S., Koons, A., Hari, D. M., Kufe, D. W., and Weichselbaum, R. R. Blockage of the vascular endothelial growth factor stress response increases the antitumor effects of ionizing radiation. Cancer Res., *59:* 3374–3378, 1999.
16. Zietman, A. L., Prince, E. A., Nakfoor, B. M., and Park, J. J. Androgen deprivation and radiation therapy: sequencing studies using the Shionogi *in vivo* tumor system. Int. J. Radiat. Oncol. Biol. Phys., *38:* 1067–1070, 1997.
17. Busse, M., and Vaupel, P. W. The role of tumor volume in "reoxygenation" upon cyclophosphamide treatment. Acta Oncol., *34:* 405–408, 1995.
18. Leunig, M., Yuan, F., Menger, M. D., Boucher, Y., Goetz, A. E., Messmer, K., and Jain, R. K. Angiogenesis, microvascular architecture, microhemodynamics, and interstitial fluid pressure during early growth of human adenocarcinoma LS174T in SCID mice. Cancer Res., *52:* 6553–6560, 1992.
19. Rockwell, P., Neufeld, G., Glassman, A., Caron, D., and Goldstein, N. *In vitro* neutralization of vascular endothelial growth factor activation of Flk-1 by a monoclonal antibody. Mol. Cell Differ., *3:* 91–109, 1995.
20. Rygaard, K., and Spang-Thomsen, M. Quantitation and gompertzian analysis of tumor growth. Breast Cancer Res. Treat., *46:* 303–312, 1997.
21. Torres Filho, I. P., and Intaglietta, M. Microvessel pO_2 measurements by phosphorescence decay method. Am. J. Physiol. *265:* H1434–H1438, 1993.
22. Tannock, I. F. Oxygen diffusion and the distribution of cellular radiosensitivity in tumours. Br. J. Radiol., *45:* 515–524, 1972.
23. Mueller-Klieser, W. Method for the determination of oxygen consumption rates and diffusion coefficients in multicellular spheroids. Biophys. J., *46:* 343–348, 1984.
24. Kallinowski, F., Zander, R., Hoeckel, M., and Vaupel, P. Tumor tissue oxygenation as evaluated by computerized-pO_2-histography. Int. J. Radiat. Oncol. Biol. Phys., *19:* 953–961, 1990.
25. Thomlinson, R. H., and Gray, L. H. The histological structure of some human lung cancers and the possible implications for radiotherapy. Br. J. Cancer, *9:* 539–545, 1955.
26. Tsai, A. G., Friesenecker, B., Mazzoni, M. C., Kerger, H., Buerk, D. G., Johnson, P. C., and Intaglietta, M. Microvascular and tissue oxygen gradients in the rat mesentery. Proc. Natl. Acad. Sci. USA, *95:* 6590–6595, 1998.
27. Helmlinger, G., Endo, M., Ferrara, N., Hlatky, L., and Jain, R. K. Growth factors: formation of endothelial cell networks. Nature (Lond.), *405:* 139–141, 2000.
28. Gullino, P. M., Grantham, F. H., Losonczy, I., and Berghoffer, B. Mammary tumor regression. III. Uptake and loss of substrates by regressing tumors. J. Natl. Cancer Inst., *49:* 1675–1684, 1972.
29. Hall, E. The oxygen effect and reoxygenation. *In:* E. Hall (ed.), Radiobiology for the Radiobiologist, Ed. 4, pp. 133–152. Philadelphia: J. B. Lippincott Company, 1994.
30. Grau, C., and Overgaard, J. Effect of cancer chemotherapy on the hypoxic fraction of a solid tumor measured using a local tumor control assay. Radiother. Oncol., *13:* 301–309, 1988.
31. Browder, T., Butterfield, C. E., Kraling, B. M., Marshall, B., O'Reilly, M. S., and Folkman, J. Antiangiogenic scheduling of chemotherapy improves efficacy against experimental drug-resistant cancer. Cancer Res., *60:* 1878–1886, 2000.
32. Klement, G., Baruchel, S., Rak, J., Man, S., Clark, K., Hicklin, D. J., Bohlen, P., and Kerbel, R. S. Continuous low-dose therapy with vinblastine and VEGF receptor-2 antibody induces sustained tumor regression without overt toxicity. J. Clin. Invest., *105:* R15–R24, 2000.
33. Rockwell, S. Oxygen delivery: implications for the biology and therapy of solid tumors. Oncol. Res., *9:* 383–390, 1997.

Tumor Oxygenation in Hormone-Dependent Tumors During Vascular Endothelial Growth Factor Receptor-2 Blockade, Hormone Ablation, and Chemotherapy

Nils Hansen-Algenstaedt, Brian R. Stoll, Timothy P. Padera, et al.

Cancer Res 2000;60:4556-4560.